

Investigation of $\text{As}_{40}\text{Se}_{60}$ chalcogenide glass in precision glass molding for high-volume thermal imaging lenses

Jeremy Huddleston, Jacklyn Novak, William V. Moreshead, Alan Symmons, Edward Foote
LightPath Technologies, Inc., 2603 Challenger Tech Ct, Ste 100, Orlando, FL, USA 32826

ABSTRACT

The growing demand for thermal imaging sensors and cameras has focused attention on the need for larger volumes of lower cost optics in this infrared region. A major component of the cost of thermal imaging lenses is the germanium content. $\text{As}_{40}\text{Se}_{60}$ was developed as a moldable, germanium-free chalcogenide glass that can serve as a low cost alternative to germanium and other infrared materials. This material also has promising characteristics for improved optical performance, especially with regard to reduced thermal sensitivity. $\text{As}_{40}\text{Se}_{60}$ has found acceptance as a material to be diamond turned or polished, but it is only now emerging as a legitimate candidate for precision glass molding. This paper will review chalcogenide molding and characterize $\text{As}_{40}\text{Se}_{60}$ for widespread use in high-volume thermal imaging optics. The relative advantages and disadvantages of $\text{As}_{40}\text{Se}_{60}$ as compared to other chalcogenide glasses will also be discussed.

Keywords: Precision glass molding, chalcogenide, thermal imaging, infrared materials, LWIR lenses

1. INTRODUCTION

Over the past decade, the prices for thermal imaging sensors have dramatically decreased through uncooled microbolometer technology. The resulting cost savings has significantly increased the demand for thermal imagers and expanded their applications in the commercial market. This in turn has increased the demand for longwave infrared (LWIR) lenses, and driven the search for high volume, low cost methods of manufacturing LWIR lenses. The technological roadmap for thermal imaging systems is following the same path that visible imaging systems have followed in the recent past; from large SLR type cameras to small handheld cameras and finally to cell phone camera systems. The enabling optical technology for the visible region was injection molding of plastic lenses. Although there are many plastic materials to choose from for the visible spectrum, these polymers absorb longwave infrared light, and are therefore inadequate for thermal applications operating in the LWIR (8-12 μm) band. Although crystalline materials such as Ge, ZnS, and ZnSe, transmit well in the LWIR band, they are not moldable and therefore they are not well-suited to high-volume, low-cost production. In recent years, chalcogenide materials have grown in popularity for LWIR lens applications. The moldability of chalcogenide glass uniquely qualifies it for the high-volume demand of commercial longwave IR applications.

Although precision glass molding (PGM) of chalcogenides has already started the trend towards low cost optics in the longwave infrared, the most commonly used chalcogenides in PGM to date have been compositions containing germanium, such as $\text{Ge}_{28}\text{Sb}_{12}\text{Se}_{60}$ (Vitron IG5) and $\text{Ge}_{22}\text{As}_{20}\text{Se}_{58}$ (Umicore Gasir 1). The push for lower cost materials and improved optical performance has caused heightened interest in the germanium-free composition $\text{As}_{40}\text{Se}_{60}$ (Vitron IG6). However, this material's availability, manufacturability, and safety must be assessed, all of which could limit its upside potential. This paper will discuss the relative advantages and disadvantages of $\text{As}_{40}\text{Se}_{60}$ as compared to the germanium-containing $\text{Ge}_{28}\text{Sb}_{12}\text{Se}_{60}$.

1.1. Overview of Precision Glass Molding

Precision glass molding, PGM, is a manufacturing process used to make high quality lenses and optical components. The general nature of the process is the compression molding of glass preforms at high temperature under highly controlled conditions. A more detailed overview of the process can be found in Schaub,et al.¹ A brief summary of the PGM process follows. The PGM process starts with the manufacturing of tooling designed specifically for the product to be manufactured. This tooling typically consists of a top mold, a bottom mold and ancillary tooling to form the outside diameter or other features of the component. Additional tooling may be required to align the individual mold halves. The customized tooling is then inserted into the glass molding machine. A glass preform is then inserted into the tooling stack. The top mold is then reintroduced and the system is evacuated. The tooling stack and the glass preform are then heated at a controlled rate. A schematic of the process is given in Figure 1.

The final processing temperature is dependent on the individual glass type. The preform is then put under compression in order to begin forming the glass. The amount of load applied to the glass is controlled throughout the molding cycle; the load is removed once the cycle is completed. The tooling stack is then cooled, typically by purging the system with an inert gas. In order to cost effectively manufacture the lens this cooling cycle is optimized for the fastest possible cycle time. Once the final product is cool enough to handle, the component is removed and the process is repeated.

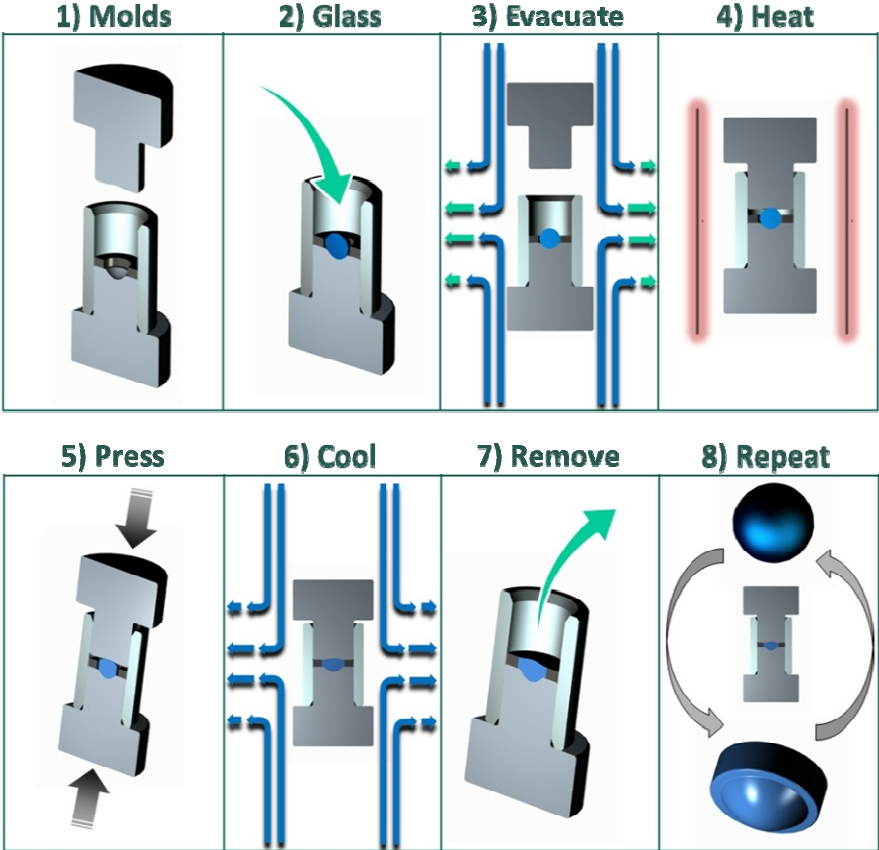


Figure 1 - Precision Glass Molding Sequence

1.2. History of Chalcogenide Glass

Chalcogenide glasses are amorphous compounds based on the chalcogen elements: sulfur (S), selenium (Se), or Tellurium (Te). One or more of the chalcogens is usually paired with at least germanium (Ge) or arsenic (As) for chemical stability. Other elements such as antimony (Sb) may be added to the composition to achieve desired properties. These glasses transmit primarily in the mid-wave infrared (MWIR) and longwave infrared (LWIR) wavebands, making them suitable for thermal imaging applications. As opposed to traditional crystalline lens materials for LWIR, such as Ge, ZnS, ZnSe, the moldability of chalcogenide glass uniquely qualifies it for the high-volume demand of commercial applications.

1.2.1. Early Use for MWIR Applications

The earliest published work on non-oxide glasses was a paper written by Carl Schulz-Sellack in 1870.^{2,3} His work showed that $As_{40}S_{60}$ chalcogenide glass was transparent in the infrared region. There was very little further research done on the subject until 1950 when the same glass composition was investigated by Rudolf Frerichs and the results were published in a paper titled “New optical glasses transparent in infrared up to $12\mu m$.”^{2,3} Frerichs’ paper renewed interest in this novel material and other groups began to research the glass. In the 1950s, $As_{40}S_{60}$ began being produced on an industrial scale and products utilizing the material were manufactured. Servo Corporation not only manufactured the glass, but also was the first to introduce a product that was made with this glass. The product was used for the detection of overheated wheel bearings on railroad cars.² The main appeal of chalcogenide glass is its infrared transparency, which makes it ideal for thermal applications.

1.2.2. Development for LWIR Applications

The transmission window of sulfide glasses only extends to about $11\mu m$, limiting it to MWIR applications. Other materials needed to be investigated in order to produce a glass with LWIR transparency. In his book, *Chalcogenide Glasses for Infrared Optics*, Hilton discusses in detail how a program at Texas Instruments (TI) was funded by the U.S. Air Force in 1966 to research infrared materials for optics. Previous research on chalcogenides had focused on electronic rather than optical properties. Hilton states that the best composition, TI 1173 ($Ge_{28}Sb_{12}Se_{60}$), was selected from the germanium-antimony-selenium system. Later research programs also investigated glasses in the germanium-arsenic-selenium system. TI produced small quantities of systems using its TI 1173 glass that were used in Air Force and Navy aircraft.² In 1977, Hilton left TI and soon founded a new company, Amorphous Materials, Inc. (AMI). Since then, they have developed and produced several “AMTIR” glasses of different compositions. Hilton notes that “during the period from 1950 to [2010], only three compositions have been produced in ton quantities: arsenic trisulfide, TI 1173 (Amtir 3), and TI 20 (Amtir 1).”²

1.3. Chalcogenide Composition Landscape

The significance of this last point is that out of the many compositions that have been developed for research purposes, only a select few have met the practical requirements of optical performance and manufacturability making them suitable for production. To highlight this point, Table 1 below shows most of the common chalcogenide compositions available from primary glass suppliers.

Table 1 - Landscape of Commercially Available Chalcogenide Glasses. The Arsenic-free and Germanium-free compositions are highlighted for their trade-offs.

Glass Composition	Notes	Brand Names from Glass Manufacturers			
		Vitron	Schott	Umicore	Amorphous Materials
$\text{Ge}_{33}\text{As}_{12}\text{Se}_{55}$		IG2	IRG22		AMTIR-1
$\text{Ge}_{30}\text{As}_{13}\text{Se}_{32}\text{Te}_{25}$		IG3	IRG23		
$\text{Ge}_{10}\text{As}_{40}\text{Se}_{50}$		IG4	IRG24		
$\text{Ge}_{28}\text{Sb}_{12}\text{Se}_{60}$	Arsenic-Free	IG5	IRG25		AMTIR-3
$\text{As}_{40}\text{Se}_{60}$	Germanium-Free	IG6	IRG26		AMTIR-2
$\text{As}_{40}\text{S}_{60}$	MWIR only				AMTIR-6
$\text{Ge}_{22}\text{As}_{20}\text{Se}_{58}$				GASIR-1	

Note that each glass supplier in Table 1 has its own brand name associated with each composition, giving the impression that there are a larger number of manufacturable compositions available than actually exist. A few important points can be taken from this table. First, all of the compositions suitable for the LWIR band contain selenium. Secondly, most are merely slight variations of the ratios in the GeAsSe family. Finally, only two of the compositions, $\text{Ge}_{28}\text{Sb}_{12}\text{Se}_{60}$ and $\text{As}_{40}\text{Se}_{60}$, stand out as containing only one of the elements germanium or arsenic. This last point has significant cost implications; both related to the rising cost of germanium, as well as the intangible cost of implementing safety procedures for arsenic-containing materials, in order to maintain a safe manufacturing work environment. For these reasons, we have chosen to focus on comparing these two chalcogenide compositions: the arsenic-free $\text{Ge}_{28}\text{Sb}_{12}\text{Se}_{60}$ and the germanium-free $\text{As}_{40}\text{Se}_{60}$.

1.4. Chalcogenide Glass for PGM

Since 2005, LightPath has conducted PGM trials with several different materials, and the arsenic-free $\text{Ge}_{28}\text{Sb}_{12}\text{Se}_{60}$ (IG5 / TI 1173 / AMTIR 3) composition was found to meet the optical performance requirements for the vast majority of applications, while providing favorable manufacturability. LightPath has branded this composition for its molded lenses as “BD2”, which can also be found in the LightPath catalog in Zemax. An assortment of these lenses can be seen in Figure 2.



Figure 2 - Molded chalcogenide glass lenses

The advantages of chalcogenides over crystalline materials such as germanium have been well documented. However, the choice between the various chalcogenide compositions has been largely subjective, based on different glass suppliers or molders marketing their particular product offerings. As discussed in the previous section, the arsenic-free $\text{Ge}_{28}\text{Sb}_{12}\text{Se}_{60}$ is a good baseline material for benchmarking the germanium-free $\text{As}_{40}\text{Se}_{60}$ composition. As such, the advantages and disadvantages of $\text{As}_{40}\text{Se}_{60}$ glass relative to $\text{Ge}_{28}\text{Sb}_{12}\text{Se}_{60}$ will be the focus of the remainder of this paper.

2. GLASS CHARACTERIZATION AND QUALIFICATION

The high volume production PGM process is critically dependent on a thorough understanding of important glass characteristics, and ensuring that these remain constant from batch to batch. Qualification of a new glass therefore involves measuring these key characteristics on glass from several batches or boules. Detailed descriptions and explanations of the techniques used for glass characterization can be found in a previous paper in reference 4, “An Investigation of Material Properties for a Selection of Chalcogenide Glasses for Precision Glass Molding.”. Although not all are discussed in detail in this paper, Table 2 shows a summary of the properties measured during qualification of $\text{As}_{40}\text{Se}_{60}$ compared to $\text{Ge}_{28}\text{Sb}_{12}\text{Se}_{60}$.

Table 2 - Key Properties of Select Chalcogenides: Arsenic-free $\text{Ge}_{28}\text{Sb}_{12}\text{Se}_{60}$ and Germanium-free $\text{As}_{40}\text{Se}_{60}$

Property	$\text{Ge}_{28}\text{Sb}_{12}\text{Se}_{60}$	$\text{As}_{40}\text{Se}_{60}$
Wavelength Range (μm)	1-16 <i>(typical absorption peak at 12.5μm)</i>	1-18
Index @ 10 μm	2.6023	2.7777
Wavelength Dispersion $dn/d\lambda$ (8-12 μm)	-3.67×10^{-3}	-2.77×10^{-3}
Thermal Constant dn/dT ($\times 10^{-6}/^{\circ}\text{C}$)	70	32
T_g ($^{\circ}\text{C}$)	285	185
CTE ($\times 10^{-6}/^{\circ}\text{C}$)	14.5	20.9
Density (g/cm^3)	4.68	4.63
Hardness (Vickers)	189	142

2.1. Optical Performance Properties

Several of the key glass properties primarily affect the optical performance of the final lens. These parameters will be discussed in this section, while the properties primarily affecting manufacturing will be discussed in section 2.2.

2.1.1. Transmission

From Table 2 we see that the wavelength ranges for both $\text{As}_{40}\text{Se}_{60}$ over $\text{Ge}_{28}\text{Sb}_{12}\text{Se}_{60}$ cover the full MWIR to LWIR band, making them suitable for thermal imaging applications. Figure 3 shows the measured transmission of both materials for uncoated witness samples. Comparing the uncoated transmission removes any differences due to AR coatings, but does include differences in reflectance from the differing refractive indices (Fresnel loss) of these materials, which is apparent in the SWIR and MWIR regions of the plot. The absorption band located at approximately $12.5\ \mu\text{m}$ is due to oxide impurities in the form of Ge-O bonds.⁵ The size of this absorption band may vary between different glass suppliers due to their processing techniques, including whether or not they have an extra purification step in their manufacturing process. $\text{As}_{40}\text{Se}_{60}$ does not contain germanium, so no Ge-O bonds can be formed and the absorption at $12.5\ \mu\text{m}$ is avoided.

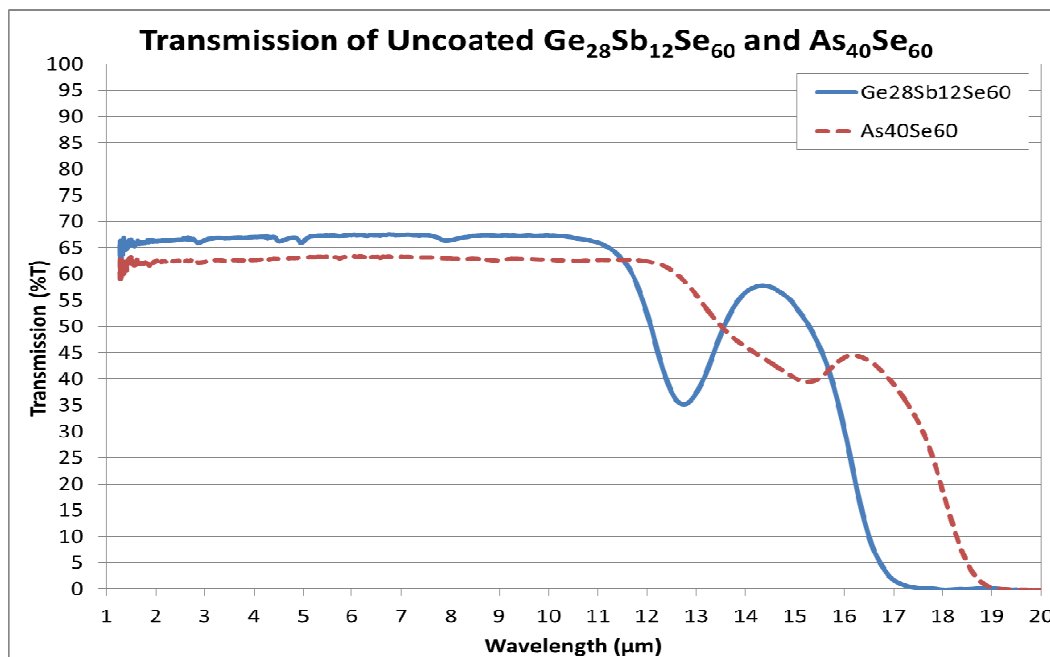


Figure 3 - Transmission of 5mm thick windows of $\text{Ge}_{28}\text{Sb}_{12}\text{Se}_{60}$ and $\text{As}_{40}\text{Se}_{60}$

2.1.2. Refractive Index

The refractive index of $\text{As}_{40}\text{Se}_{60}$ is higher than that of $\text{Ge}_{28}\text{Sb}_{12}\text{Se}_{60}$ and therefore more optical power may be achieved on a given lens for the same sag and slope limitations. However, this difference is small compared to the index differences between other LWIR materials, and therefore does not constitute a significant advantage for $\text{As}_{40}\text{Se}_{60}$. It will be shown in section 4 that approximately the same nominal performance can be achieved for both lens materials.

2.1.3. Wavelength Dispersion

Figure 4 shows the overlaid plots of refractive index vs. wavelength for $\text{As}_{40}\text{Se}_{60}$ compared to $\text{Ge}_{28}\text{Sb}_{12}\text{Se}_{60}$. The wavelength dispersion, or change in refractive index with wavelength ($dn/d\lambda$) is indicated by the slopes of these curves. In the MWIR, the dispersion of these two materials is approximately equal, but the dispersion in the LWIR band is slightly lower for $\text{As}_{40}\text{Se}_{60}$. Though small, this difference represents an incremental advantage in nominal performance for $\text{As}_{40}\text{Se}_{60}$. However, diffractive elements are often added to chalcogenide lenses to compensate for wavelength distortion. In most cases, this obviates any perceived advantage to lower material dispersion, which is verified in the design study of section 4.

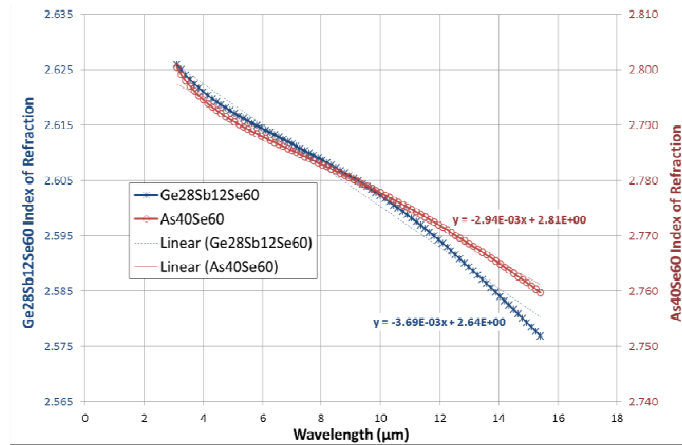


Figure 4 - Wavelength dispersion of $\text{Ge}_{28}\text{Sb}_{12}\text{Se}_{60}$ (left axis) and $\text{As}_{40}\text{Se}_{60}$ (right axis)

2.1.4. Thermal Sensitivity

The thermal coefficient of refractive index, or dn/dT , is the change in refractive index over temperature. Figure 5 shows the measured data for the refractive index vs. temperature of $\text{As}_{40}\text{Se}_{60}$. The lower thermal constant of $\text{As}_{40}\text{Se}_{60}$ (32ppm/ $^{\circ}\text{C}$) theoretically enables a higher intrinsic operating temperature range relative to $\text{Ge}_{28}\text{Sb}_{12}\text{Se}_{60}$. The practical effect of this constant on MTF performance over temperature has been shown⁶ (by the present authors in a previous paper) to be inadequately described by first-order optical theory, and lacks a consistent performance criterion across the industry, even for rigorous MTF analyses. Assessing this impact will be the primary focus of the design study in section 4.

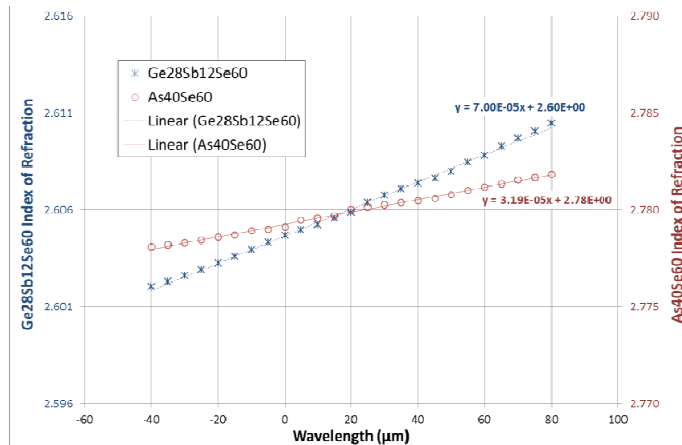


Figure 5 - Refractive index vs. Temperature of $\text{Ge}_{28}\text{Sb}_{12}\text{Se}_{60}$ (left axis) and $\text{As}_{40}\text{Se}_{60}$ (right axis)

2.2. Mechanical Properties

Beyond the optical characteristics of $As_{40}Se_{60}$, other mechanical properties were measured for validating glass quality and compatibility with manufacturing requirements.

2.2.1. Composition

The composition of $As_{40}Se_{60}$ was measured using Proton-Induced X-Ray Emission (PIXE) on fine-ground discs of the chalcogenide glass, and the results are shown in Table 3.

Table 3 - Measured Composition of $As_{40}Se_{60}$ Glass

Element	Atom %	Error (%)
Arsenic	40.1	0.4
Selenium	59.9	0.6

2.2.2. Thermal Properties

The thermal properties of a glass must be well understood for compatibility with the PGM process. LightPath thoroughly investigates these properties in order to choose the best processing temperatures, materials, and techniques. Dilatometry was used to measure the coefficient of thermal expansion (CTE), dilatometric glass transition temperature $T_{g(dil)}$, and the softening point. The results are shown in Figure 6.

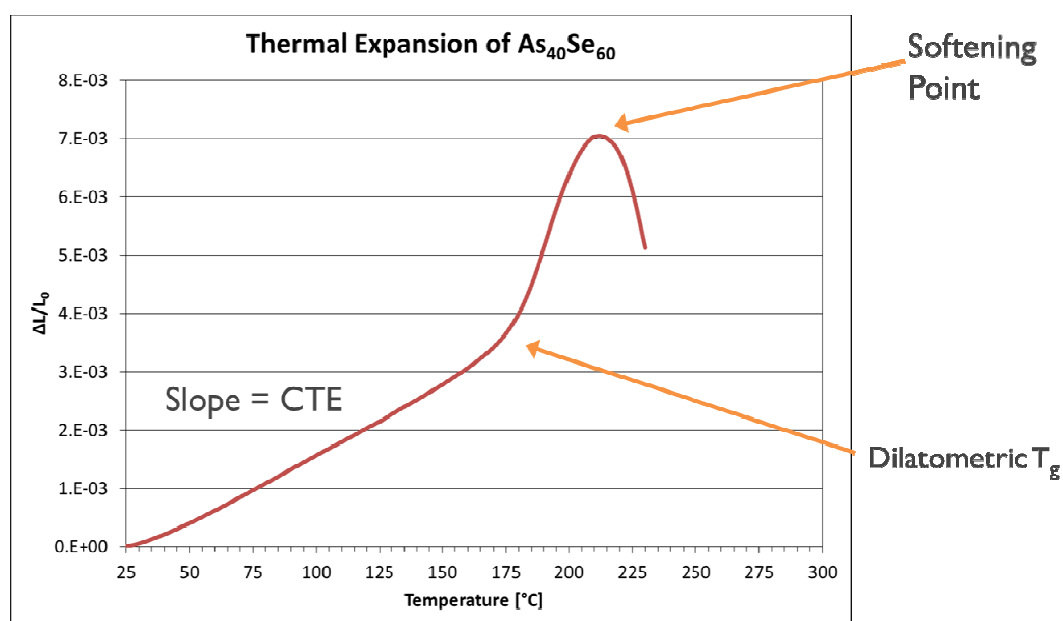


Figure 6 - Dilatometry curve of $As_{40}Se_{60}$ sample

The shape of the curve and the values of CTE, $T_{g(dil)}$, and the softening point are all dependent on the heating rate used in the experiment, which was $3^\circ C/min$ for this sample. From the curve, we find that the CTE from 25-100°C is $20.9 \times 10^{-6} / ^\circ C$, $T_{g(dil)}$ is $175^\circ C$, and the softening point is $210^\circ C$.

Referencing Table 2, we see that the CTE of $\text{As}_{40}\text{Se}_{60}$ is slightly higher than $\text{Ge}_{28}\text{Sb}_{12}\text{Se}_{60}$, which has implications on both molding and the optomechanical design of lens assemblies. Due to the elevated temperatures of the molding process, even moderate differences in CTE can have significant effects on press yields. The geometries of the preforms and molds must all be analyzed and balanced for optimal forming of the final lens shape and proper release from the mold. Also, the most commonly used lens housing material for LWIR applications is aluminum, which has a CTE of $23\text{ppm}/^\circ\text{C}$. This means that $\text{As}_{40}\text{Se}_{60}$ is a closer match to Al than $\text{Ge}_{28}\text{Sb}_{12}\text{Se}_{60}$ which can improve the thermal stability of the full lens assembly.

In the case of dilatometry, the $T_{g(\text{dil})}$ is the temperature where the CTE departs from the typical linear relationship. The T_g can also be determined using differential scanning calorimetry (DSC) and, in this case, it is determined by finding the onset of a change in heat flow. A DSC curve for $\text{As}_{40}\text{Se}_{60}$ is shown in Figure 7. The heating rate used was $10^\circ\text{C}/\text{min}$ in this experiment.

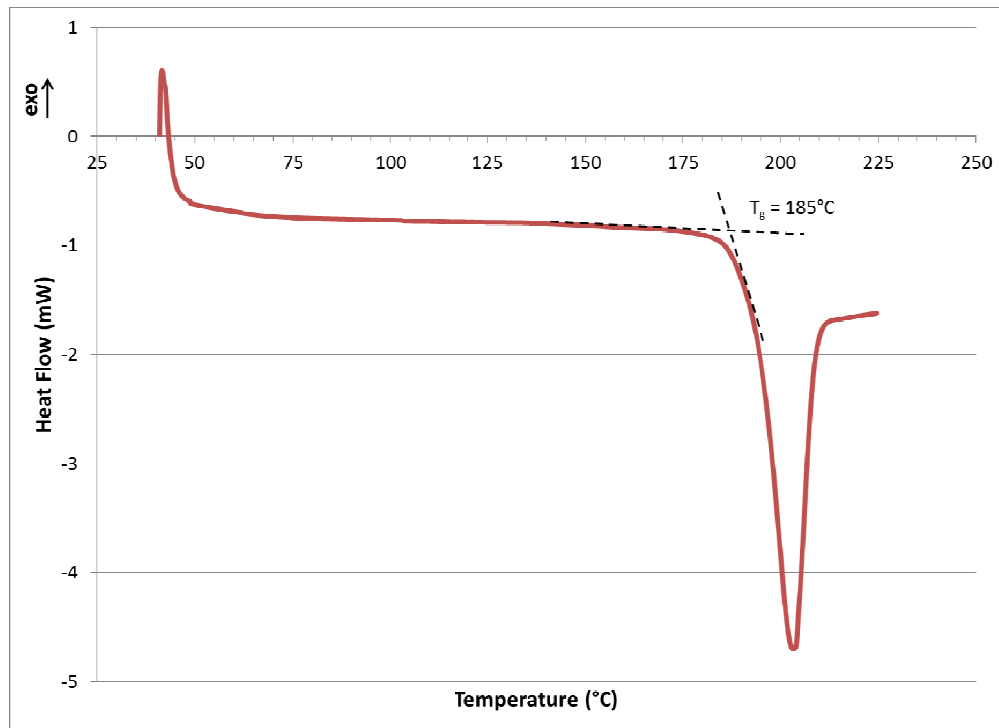


Figure 7 - Determination of the T_g from the DSC curve of an $\text{As}_{40}\text{Se}_{60}$ sample

The glass transition temperature of $\text{As}_{40}\text{Se}_{60}$ is 100°C lower than that of $\text{Ge}_{28}\text{Sb}_{12}\text{Se}_{60}$. This lower T_g can be an advantage in the molding process, since lower molding temperatures are required. Molds are expected to last longer, and in general glass interactions with molds are expected to be less. However, this lower T_g could be a limiting factor for some applications if high temperature stability is an issue.

2.2.3. Density

Density can be important when the weight of an optical assembly is critical, e.g. space or head-mounted applications. As shown in Table 2, the density of $\text{As}_{40}\text{Se}_{60}$ is not significantly different from that of $\text{Ge}_{28}\text{Sb}_{12}\text{Se}_{60}$. In this case, the germanium-free glass does not present an advantage or disadvantage.

2.2.4. Hardness

The microhardness of the chalcogenide glasses was measured with a Vickers diamond indenter. While the values reported for both glasses in Table 2 are lower than traditional crystalline materials, hard carbon (diamond-like) coatings have been developed to improve the material's durability when required for certain applications. $As_{40}Se_{60}$ is significantly softer than $Ge_{28}Sb_{12}Se_{60}$, while this does not have a significant impact on the molding performance, it does have ramifications across the supply chain. Softer preforms are much more difficult to manufacture and handle and finished lens are easier to scratch and damage and more difficult to coat. The cost savings associated with removing the Ge, can be offset by increased processing costs and lower yields.

2.3. Intangible Considerations for High Volume Production

On the surface, $As_{40}Se_{60}$ offers the potential for several advantages over $Ge_{28}Sb_{12}Se_{60}$, both in performance and reduced cost from the absence of germanium. In practice, however, there are intangible limitations to realizing these advantages.

First, the cost of a germanium-free composition is theoretically less expensive, but the supply chain must be established and stabilized for high volumes as has been achieved for $Ge_{28}Sb_{12}Se_{60}$. Since $As_{40}Se_{60}$ is in the early stages of use compared to $Ge_{28}Sb_{12}Se_{60}$, these cost savings have yet to be realized by primary glass suppliers.

Another consideration is that arsenic-containing compounds must be carefully handled in any manufacturing environment, and appropriate safety precautions must be implemented. This can lead to increased overhead costs in manufacturing.

Finally, lower press temperatures may predict longer mold lifetimes and better yields, but those yields must be validated through process optimization, and they must actually be maintained in volume production.

Such reservations may seem overly cautious, but because it is difficult to quantify their true impact on cost, they are easily overlooked or disregarded.

3. MOLDING QUALIFICATION RESULTS

After careful characterization of the $As_{40}Se_{60}$ material, trial lenses were pressed with preliminary optimization of molding conditions. Figure 8 shows an image of 2 of the molded lenses.



Figure 8 - Image of Successfully Molded $As_{40}Se_{60}$ Lenses

100% of the lenses in this feasibility trial pressed successfully and passed the same MTF criteria as a similar $\text{Ge}_{28}\text{Sb}_{12}\text{Se}_{60}$ lens that had been designed to the same performance specification. Figure 9 shows the measured MTF results (average and standard deviation error bars) of the comparable designs in $\text{As}_{40}\text{Se}_{60}$ and $\text{Ge}_{28}\text{Sb}_{12}\text{Se}_{60}$.

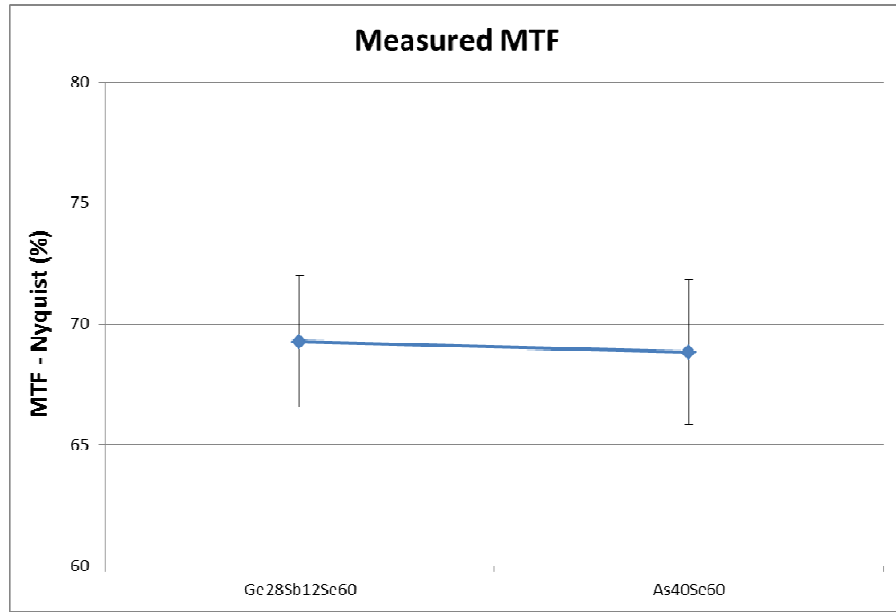


Figure 9 - Measured On-axis MTF for $\text{As}_{40}\text{Se}_{60}$ and $\text{Ge}_{28}\text{Sb}_{12}\text{Se}_{60}$ Lenses

The form error of the lenses was also analyzed for both the deviation in radius of curvature and the RMS irregularity. Because the molds can be adjusted to dial in accuracy, the variation from lens to lens is the key parameter to assess for molding stability. Figure 10 shows that the variation in measured form error is comparable, and even lower on $\text{As}_{40}\text{Se}_{60}$ lenses relative to $\text{Ge}_{28}\text{Sb}_{12}\text{Se}_{60}$ lenses.

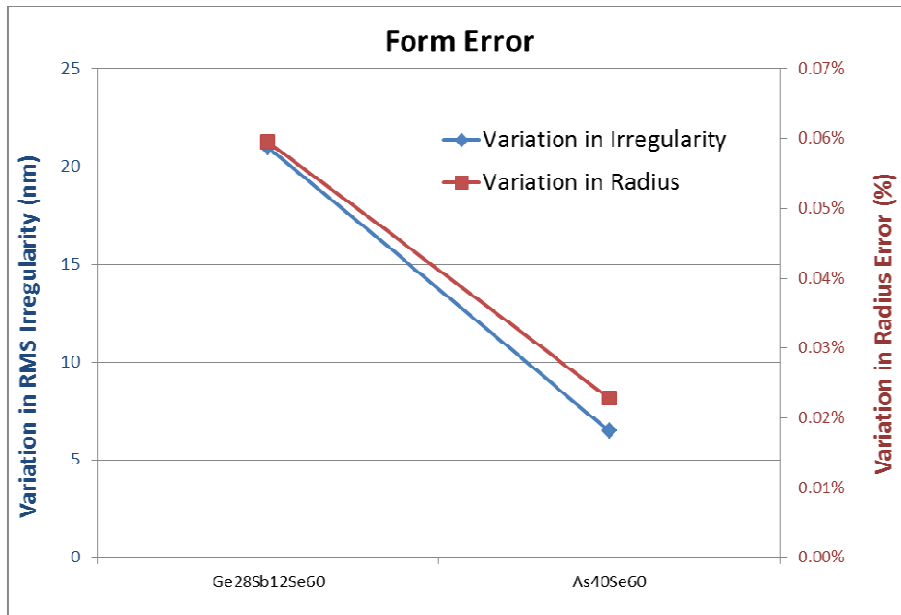


Figure 10 - Measured Variation in Form Error for $\text{As}_{40}\text{Se}_{60}$ and $\text{Ge}_{28}\text{Sb}_{12}\text{Se}_{60}$ Lenses

4. THERMAL DESIGN STUDY

Because one of the key differences between $As_{40}Se_{60}$ and $Ge_{28}Sb_{12}Se_{60}$ is the thermal sensitivity (dn/dT), it is important to determine the performance impact of this difference in a practical design scenario. It has been shown in a previous paper by the present authors that first-order approximations in athermalization theory are inadequate for accurately determining the practical performance impact of the material thermal constant.⁶ In that study, a singlet was designed in several LWIR materials (including $As_{40}Se_{60}$ and $Ge_{28}Sb_{12}Se_{60}$) and the MTF sensitivity to operating temperature was determined. Though these differences in MTF performance did not match first-order theory, they were still significant in differentiating lens materials for use in LWIR imaging systems. The singlet design case study found that $As_{40}Se_{60}$ was approximately half as sensitive to temperature as $Ge_{28}Sb_{12}Se_{60}$.⁶

In this paper, we seek to extend that design study to the case of 2-element lens systems. Because there are many more design forms possible for a 2-element system, we began with a nominal design survey to determine the design forms that were least sensitive to tolerances for a given set of constant performance constraints. This study considered a 9mm efl lens with an F-number of 1.0 and a 24deg FOV. After the most tolerant design form was determined, independent of material, the materials were interchanged and re-optimized with the same performance constraints. The designs were then compared for thermal sensitivity *in the absence of any mechanical athermalization*, the results of which are found in Table 4 and Figure 11.

Table 4 - 2-Element Design Study with (left) material combinations, (center) nominal MTF, and (right) MTF over -40 to 85°C

	Lens Material		Nominal MTF			Min MTF over -40 to 85°C		
	Lens 1	Lens 2	On-axis	HFOV	Corner	On-axis	HFOV	Corner
1	$Ge_{28}Sb_{12}Se_{60}$	$Ge_{28}Sb_{12}Se_{60}$	42%	40%	38%	19%	13%	9%
2	$Ge_{28}Sb_{12}Se_{60}$	$Ge_{28}Sb_{12}Se_{60}$	42%	39%	37%	22%	17%	16%
3	$Ge_{28}Sb_{12}Se_{60}$	$Ge_{28}Sb_{12}Se_{60}$	42%	39%	37%	23%	15%	13%
4	$Ge_{28}Sb_{12}Se_{60}$	$Ge_{28}Sb_{12}Se_{60}$	42%	39%	38%	16%	15%	16%
5	$As_{40}Se_{60}$	$As_{40}Se_{60}$	42%	41%	39%	39%	36%	35%
6	$As_{40}Se_{60}$	$Ge_{28}Sb_{12}Se_{60}$	42%	40%	39%	33%	27%	27%
7	$Ge_{28}Sb_{12}Se_{60}$	$As_{40}Se_{60}$	42%	39%	37%	34%	27%	27%
8	Ge	$Ge_{28}Sb_{12}Se_{60}$	42%	40%	39%	7%	0%	0%
9	ZnSe	$Ge_{28}Sb_{12}Se_{60}$	42%	36%	34%	24%	15%	14%
10	ZnSe	$As_{40}Se_{60}$	41%	36%	33%	35%	29%	28%

The first 4 designs of Table 4 show different design forms, all using the same $Ge_{28}Sb_{12}Se_{60}$ material for both lens elements. The differences in nominal performance (center 3 columns) are minor, though the temperature sensitivity differences are slightly more noticeable amongst these 4 designs. Design 5 represents the $As_{40}Se_{60}$ version of the best 2-element design form. Finally, the remaining designs represent hybrid combinations of different lens materials for each of the 2 elements in the system. Only the designs containing ZnSe had a significantly lower nominal MTF, though only for the off-axis fields. This is primarily due to the lower refractive index of ZnSe. When examining the MTF over temperature in the right 3 columns, several groupings stand out. The design using $As_{40}Se_{60}$ is by far the least sensitive to temperature. Those hybrid designs containing $As_{40}Se_{60}$ show slightly higher sensitivity. The designs containing $Ge_{28}Sb_{12}Se_{60}$ but not $As_{40}Se_{60}$ are more sensitive still. Finally, by far the most sensitive design is the one containing Ge, due to its dn/dT value of $\sim 400\text{ppm}/^\circ\text{C}$, which is more than 5 times higher than the dn/dT of $Ge_{28}Sb_{12}Se_{60}$. These groupings are more easily seen in Figure 11, which plots the same data represented in Table 4.

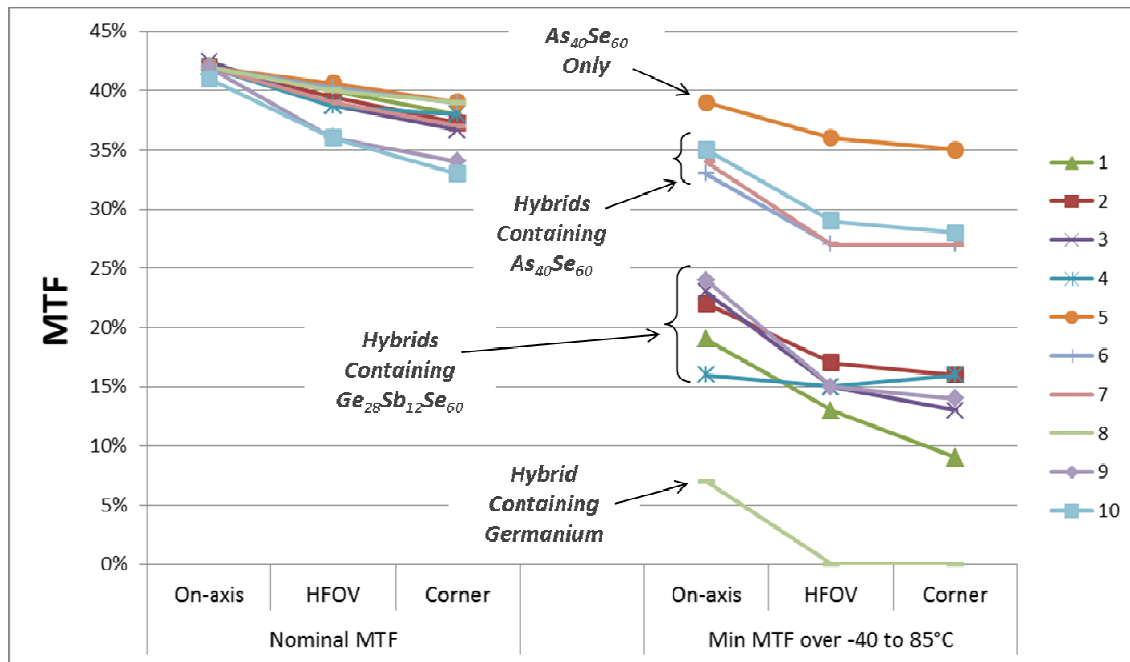


Figure 11 - Data from Table 4: (left) nominal MTF and (right) MTF over -40 to 85°C

This 2-element design study further accentuates the advantage $As_{40}Se_{60}$ brings to optical athermalization. Although the referenced singlet design study concluded that $As_{40}Se_{60}$ may still require some mechanical athermalization, this 2-element design study shows that $As_{40}Se_{60}$ brings significantly improved athermal performance that could allow for removal of any mechanical athermalization.

5. CONCLUSIONS

Chalcogenide lenses are increasingly becoming the lens material of choice for thermal imaging applications due to their unique properties as moldable materials with high transmission in the LWIR band. These properties enable high volume PGM manufacturing with high performance at relatively low costs. Although germanium-containing compositions have been the primary materials used to date, $As_{40}Se_{60}$ offers promising potential for improved thermal performance and lower cost for high volume consumer applications. However, these potential advantages must be carefully weighed against potential supply chain, safety and yield requirements. With both germanium-free and arsenic-free compositions to choose from, LightPath is well-positioned to be the PGM lens supplier of choice for the LWIR market.

ACKNOWLEDGEMENTS

The authors of this paper would like to thank the Infrared Development team at LightPath Technologies for their contributions to this paper. All figures courtesy of LightPath Technologies Inc.

REFERENCES

- ¹ Schaub, M., Schwiegerling, J., Fest, E.C., Symmons, A., and Sheppard, R.H. *Molded Optics: Design and Manufacture*, "Chapter 5: Molded Glass Optics." CRC Press, Taylor and Francis Group, London (2011).
- ² Hilton Sr., A.R. *Chalcogenide Glasses for Infrared Optics*. McGraw-Hill Companies (2010).
- ³ Popescu, M.A. *Non-Crystalline Chalcogenides*. Kluwer Academic Publishers (2000).
- ⁴ Moreshead, W.V., Novak, J., and Symmons, A. "An Investigation of Material Properties for a Selection of Chalcogenide Glasses for Precision Glass Molding," *Electro-Optical and Infrared Systems: Technology and Applications IX*, edited by David A. Huckridge, Reinhard R. Ebert, Proc. of SPIE Vol. 8541, 854102 (2012).
- ⁵ Kokorina, V.F., *Glasses for Infrared Optics*, CRC Press, Inc. (1996).
- ⁶ Huddleston, J., Symmons, A., and Pini, R. "Comparison of the thermal effects on LWIR optical designs utilizing different infrared optical materials," Proc. of SPIE Vol. 9070, 90702E (2014).